Quantitative assessment of the impacts of irrigation on surface water fluxes in the Tarim River, China

Zhenchun Hao, Sichun Chen, Zehua Li, Zhongbo Yu, Quanxi Shao, Fei Yuan and Fangxin Shi

ABSTRACT

Irrigation is a significant human activity that affects surface water fluxes in the Tarim River Basin. To quantitatively assess the irrigation impact of this activity on surface water fluxes in the Tarim River, a land surface hydrologic model was coupled with a modified irrigation scheme and a reservoir module and applied to simulate these fluxes. Modeling results indicate that the combined effect of the irrigation process and reservoir operation is prominent in the study area, from which 70–75% of the surface water is extracted and used for irrigation. This scenario can primarily be attributed to the significant amount of water losses as a result of evaporation and the seepage of canals and aqueducts. The effective utilization coefficient of the extracted surface water is only approximately 0.40. The irrigation water withdrawals increased with the recent rapid expansion of cultivated land. Therefore, the water flowing into the main stem of the Tarim River still shows a downward trend, despite the significant increase in the total discharge of headwater basins since the 1960s.

Key words | irrigation impact, oasis agriculture, surface water fluxes, Tarim River

Zhenchun Hao
Sichun Chen
Zehua Li (corresponding author)
Zhongbo Yu
Fei Yuan
Fangxin Shi
State Key Laboratory of Hydrology-Water Resources and Hydraulic Engineering,
Hohai University,
Nanjing 210098,
China
E-mail: *lizh_hhu@live.com*

Quanxi Shao
CSIRO Computational Informatics,
Private Bag 5, Wembley, WA 6913,
Australia

INTRODUCTION

The problem of over-abstraction in surface water has been well documented (Shiklomanov & Rodda 2003). It is commonly exacerbated in combination with extended natural dry periods. Substantive reductions in major river flows have been noted worldwide, along with significant reductions in the size and volume of lakes and inland sea areas (Postel 2000; Vörösmarty *et al.* 2000). These problems are typically tied closely to upstream diversions and reservoirs in some large river basins, especially those in parts of Asia and in the western United States, where humans directly alter the dynamics of the water cycle through dams constructed for water storage and through water withdrawals for agricultural purposes (Haddeland *et al.* 2013). Moreover, water-intensive farming and irrigation enhance evapotranspiration and reduce runoff. Awareness regarding the effect of irrigation on the surface water balance is increasingly important in arid and semi-arid regions in northwestern China (Hao *et al.* 2008; Tao *et al.* 2008). The most prominent example of an affected region is the Tarim River Basin (TRB), which is the largest inland river basin in China. Many of the causes of this effect persist despite years of over-use changes in both water and related ecosystem conditions. These causes include highly inefficient water supply provision practices to expand oasis agriculture use and a basic lack of control over water source exploitation. The inappropriate development of reservoirs and diversions has complicated and enhanced the impacts on existing water resources and ecosystems in the TRB.

A number of studies have focused on the impacts of climate change and human activities on water resources in the TRB. Xu *et al.* (2010) detected the long-term trend of the hydrological time series, including air temperature, precipitation, and streamflow, using both parametric and nonparametric techniques. They concluded that although the precipitation and streamflow from the headwaters of the Tarim River increased significantly as a result of climate change, the streamflow displays a decreasing trend along the main stem. This observation may be attributed to the effect

doi: 10.2166/nh.2015.215

of human activities. Liu & Chen (2006) collected time series data on population change, economic development, climate change, water volume and quality, and changes in oasis land use to study the interactions between these factors in the TRB. The results imply that human activity, rather than climate change, dominates the recent environmental changes in the basin. Tao *et al.* (2011) revealed that the local human activities starting from the 1970s have reduced the water volume diverted into the main stem. This reduction was aggravated in the 2000s based on a comparison of the total discharge of the four headstreams in the mountains and of the discharge flowing into the main stem of the Tarim River. Most of the previous studies attempted to examine the trends in hydro-climatic variables and to explain the relationship between these variables using statistical techniques. However, the methods used lack a physical basis in human activities such as irrigation withdrawal and related reservoir operation, both of which dominate the surface water fluxes in the TRB. Thus, we still know very little about their impacts on surface water fluxes in space and time, as well as their background mechanisms.

Some recent studies have analyzed the effects of irrigation on surface water and energy fluxes using large-scale hydrological models and land surface schemes. Döll & Siebert (2002) used a model of global water resources and water use, to compute global irrigation requirements under present-day climate. Boucher *et al.* (2004) represented the effect of irrigation in a general circulation model by incorporating the increase in evapotranspiration caused by irrigation in idealized climate simulations. de Rosnay *et al.* (2003) developed an irrigation scheme for a land surface model to estimate the increase in latent heat flux over the Indian Peninsula. Fekete *et al.* (2010) used a water balance model to compare the impacts of human water consumption and those of the expected climate changes on annual runoff over the next decades. An irrigation scheme based on simulated soil moisture deficit and available water was developed in the land surface hydrologic model to predict irrigation water demands and actual water withdrawals (Haddeland *et al.* 2006a). Unlike other approaches, this model considers the effects of dams and reservoirs using a reservoir module. Hence, water can be stored for later use. This model has been successfully implemented to reproduce irrigation effects on surface water fluxes at the regional, continental, and global scale (Haddeland *et al.* 2006a, b, 2013). However, the direct use of the model is problematic given that its irrigation scheme does not represent water supply efficiency, which is very low in the TRB (Zhou *et al.* 2000). To address this issue, the current paper presents an improved irrigation system. It mainly differs from the original irrigation scheme in that it also estimates irrigation water demands, actual water withdrawals, and water losses using a generalization algorithm and based on a prescribed effective utilization coefficient.

In this study, we address the question of whether and how irrigation impacts surface water fluxes by using a coupled version of the land surface hydrologic model (Liang *et al.* 1994; Haddeland *et al.* 2006a). A related question is regarding how the impacts have changed in recent decades. The following section describes the selected study site and datasets. The third section explains the model construction in detail and focuses on the modification to the model. The fourth section presents the results, including model performance, irrigation impacts on surface water fluxes, and their changing trends. The fifth section discusses the results with respect to the applied method and provides conclusions and recommendations for further research.

STUDY SITE AND DATASETS

Study site

The 1,321 km long Tarim River is China's longest inland river. The TRB has an area of over 1 million km^2 and covers the entire southern part of the Xinjiang Uyghur Autonomous Region (Figure 1). It is bordered by the Tianshan, Pamir, and Kunlun mountain ranges, all of which cut off humid air currents from the Indian Ocean and Atlantic Ocean. Thus, the climate is extremely arid, and the mean annual precipitation in this area is less than 100 mm. In addition to orographic rainfall, snow and glacier melts contribute significantly to the runoff. Irrigation agriculture is concentrated in the oasis along the foothills of the mountains. The existing oasis was enlarged and a large area of virgin land was opened to agriculture in the 1950s. Cotton gradually replaced wheat as the major crop in Xinjiang,

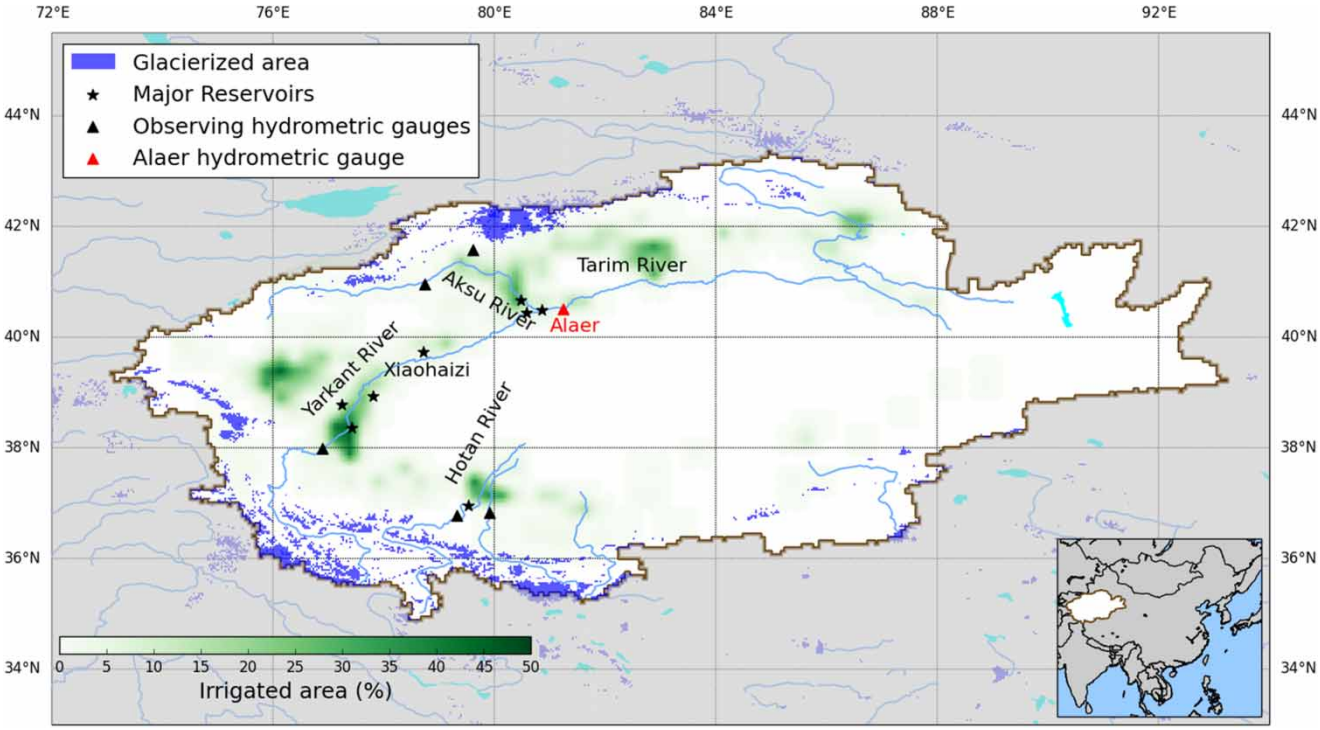

Figure 1 | Location of the Tarim River Basin.

and this province has become the largest cotton producer in China. This resulted in steadily increasing water demands along the Tarim River and its tributaries because all agriculture depends on irrigation. To satisfy the increasing water demands, a series of water diversion and storage projects was implemented to store and provide water for irrigation use. Most of these projects target the depression and the lower part of the alluvial plains (Thevs 2011). Only three water systems maintain a natural hydraulic relationship with the mainstream, namely, the Aksu River, which originates from the Tianshan Mountains; the Hotan River from the Kunlun Mountains; and the Yarkant River located between the first two rivers. The Hotan River is usually dry as it has to cross the Taklamakan Desert to get to the Tarim River. For this reason, the Hotan River as an ephemeral stream, and is not linked with Alaer in Figure 1. The Kaidu River also transports water to the lower reaches of the Tarim River from Bosten Lake on occasion. Thus, these four rivers form the headwater streams that feed the Tarim River and are important in the agricultural production, socio-economic development, and ecological conservation of the TRB (Chen *et al.* 2009).

Datasets

In this study, the air temperature is gridded from observations following methods outlined in Xu *et al.* (2009) and precipitation is a gridded dataset from the Asian Precipitation-Highly Resolved Observational Data Integration Towards Evaluation of Water Resources (APHRODITE) project (Yatagai *et al.* 2012). Wind speed is derived and gridded from NCEP-NCAR reanalysis (Sheffield *et al.* 2006). They are combined as meteorological forcing data at a spatial resolution of half degree from 1961 to 2007 to drive the model. Figure 2 shows the spatial distribution of annual average air temperature and precipitation in the TRB. The air temperature increases from the surrounding mountains to the central desert of the basin, with an annual average of 4.9 °C. Precipitation increases inversely, with an average of 83.3 mm. The monthly mean temperature ranges from −12 °C in January to 18.5 °C in July. More than 80% of the total precipitation falls between May and September, while the rest falls from November to the following April. The headwater streams within the TRB are supplied by snow melt, glacier melt, and summer rainfall in the Kunlun, Pamir, and

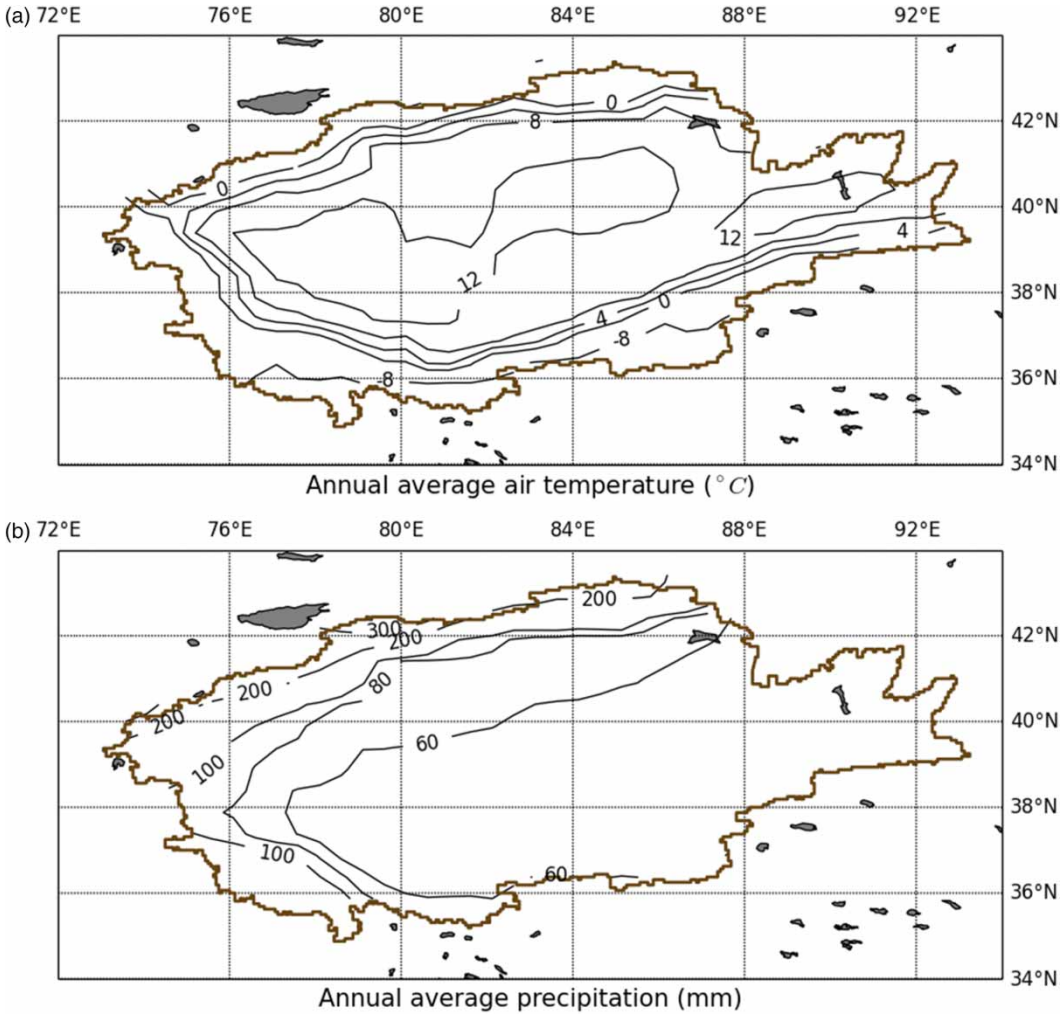

Figure 2 | Contours of annual average temperature and precipitation in the Tarim River Basin.

Tianshan Mountains. In particular, snow melt contributes considerably to the spring-time runoff of the Tarim River. When the air temperature in the high mountains increases in the summer, glacier melt water and orographic rainfall become the major runoff sources. Three-quarters of the annual runoff are concentrated in the summer season.

As indicated above, most of the streamflow originates from the snow melt, glacier melt, and orographic rainfall in the mountainous areas around the TRB. To effectively estimate the surface water fluxes over the irrigated area, the discharge data from 1961 to 2007 observed at the five hydrometric gauges monitored by the Xinjiang TRB Management Bureau were selected as part of the routing model inputs. The hydrometric gauges are located upstream of the reservoir system and the irrigated area (Figure 1). In addition, information on a series of major reservoirs operated by a local agency is collected to parameterize the reservoir module, which is included in the routing model. Detailed information on the hydrometric gauges and reservoirs is listed in Tables 1 and 2.

MODEL CONSTRUCTION

Land surface hydrologic model

The physically based, semi-distributed variable infiltration capacity (VIC) model was used to derive soil moisture over the study area. Liang *et al.* (1994) described the

Table 1 | Detailed information on the observing hydrometric gauges in the headstreams of the Tarim River Basin

Water system	Hydrometric gauges	Drainage area (km^2)	Latitude	Longitude
Aksu River	Xiehela	12,816	41° 34′ N	79° 37′ E
	Shaliguilanke	17,898	40° 57′ N	78° 36′ E
Hotan River	Tongguziluoke	14,575	36° 49′ N	79° 55′ E
	Wuluwati	15,557	36° 57′ N	79° 41′ E
Yarkant River	Kaqun	48,100	37° 59′ N	76° 54′ E

formulation of the VIC model with two soil layers in detail; thus, we provide only a brief introduction in this section. A third soil layer was added by Liang *et al.* (1996) to improve the evapotranspiration predictions in arid climates, and the VIC model solves the water and energy balance equations given the land surface over each grid cell (half degree in this case). Subgrid variability in topography, vegetation, and precipitation is represented in the form of a mosaic, wherein each grid cell is partitioned into elevation bands. Each band contains a number of land cover tiles. The soil column is divided into multiple layers (typically three). The saturation excess mechanism, which produces surface runoff, is parameterized through the Xinanjiang variable infiltration curve (Zhao 1992). Drainage from the lowest soil layer is controlled through a non-linear recession curve (Nijssen *et al.* 2001).

Irrigation scheme and reservoir module

Haddeland *et al.* (2006a) proposed an irrigation scheme to accommodate irrigation water withdrawals in the VIC model based on the modeled soil moisture deficit and available water. The irrigation process within the scheme is designed to begin when soil moisture of the top layer drops below the level at which transpiration is limited and continues until soil moisture reaches field capacity. The grid cells in which irrigation occurs are partitioned into irrigated and non-irrigated parts (Figure 3(a)) according to Siebert *et al.*'s (2002) dataset on the fractional area irrigated with the cell. Vegetation has changed

Table 2 | Detailed information on major reservoirs in the Tarim River Basin

Reservoir	Year of construction	Height of dam (m)	Storage of reservoir (10^6 m^3)	Surface area (km^2)	Latitude	Longitude
Shengli	1970	5	108	51.6	40° 15′ N	80° 45′ E
Shangyou	1961	5	180	136.5	40° 15′ N	80° 45′ E
Duolang	1965	5	128	48.0	40° 45′ N	80° 45′ E
Xiaohaizi	1960	16	872	145.0	39° 45′ N	78° 45′ E
Sukuqiake	1985	5	281	133.6	38° 45′ N	77° 15′ E
Yiganqi	1956	6	166	47.2	38° 15′ N	77° 15′ E
Qianjin	1969	6	127	45.0	38° 45′ N	77° 15′ E
Wuluwati	2001	132	347	13.0	37° 15′ N	79° 45′ E

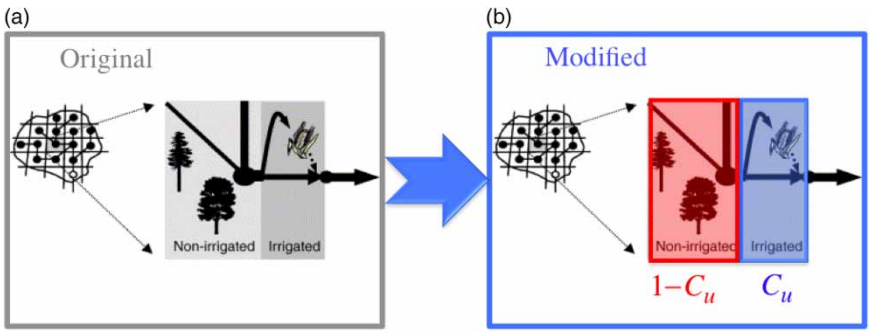

Figure 3 | Schematic of the VIC irrigation scheme. (a) Original (Haddeland *et al.* 2006a); (b) modified.

considerably along with agricultural expansion in recent decades; thus, a dataset of irrigated area with decadal change was generated as the VIC input by combining Siebert *et al.*'s (2002) dataset with that presented by Liu & Chen (2006). Crop characteristics are determined based on the AQUASTAT database of the Food and Agriculture Organization (FAO; www.fao.org/ag/agl/aglw/aquastat/main). Reference crop evapotranspiration is first calculated within each model grid cell based on the Penman–Monteith method (Monteith 1965). The crop coefficients and heights specified by FAO are thereafter used to calculate the values of the leaf area index throughout the growing season. The crops with these characteristics are assigned to the irrigated part of the grid cell, while the remaining vegetation is assigned to the non-irrigated part. Given that a series of reservoirs has been built in the TRB for irrigation purposes, the irrigation process and reservoir operation are combined to dominate the surface water fluxes in this area. A generic reservoir module was therefore incorporated into the routing model presented by Lohmann *et al.* (1998). In the reservoir module, the operation of the dams presumably follows simple rule curves, which are constructed based on irrigation water demands in the study area. An optimization scheme based on the shuffled complex evolution metropolis algorithm (Vrugt *et al.* 2003) was used to calculate optimal releases given the reservoir inflow, storage capacity, and downstream water or power demands (Haddeland *et al.* 2006b). Irrigation water is extracted in order of priority from the local runoff, river discharge, and from reservoirs in periods of water scarcity. This water is returned to the soil column to sustain crop growth as necessary.

In order to carry out water withdrawals correctly, this coupled version of VIC model was rewritten to run from upstream to downstream locations in a basin. In this way, the routing model is allowed to interact with the VIC model, and is no longer simply a post-processing step. In the original version of the irrigation scheme (Haddeland *et al.* 2006a), the canals and aqueducts built for irrigation water transport were excluded from the modeling scheme. As a result, actual irrigation water withdrawals are underestimated because of possible irrigation water loss from these structures. According to an observation-based study on the surface water supply efficiency in the TRB (Zhou *et al.* 2000), the effective utilization coefficient of surface water is low because of intense evaporation and the seepage from canals, aqueducts, and reservoirs. Directly using the original irrigation scheme in the TRB is problematic. To address this issue and to consider these considerable water losses, we present an improved irrigation scheme. This scheme not only estimates irrigation water demands, actual water withdrawals, and actual water losses based on simulated soil moisture deficit and available water, but also through an effective utilization coefficient (C_u), which is prescribed by a generalization algorithm. This scenario indicates that the withdrawn irrigation water returns to the soil column of the irrigated area only partially to sustain the crops, while the rest is assigned to the non-irrigated area as a loss term (Figure 3(b)). Specifically, irrigation water demand is defined as the amount of water demanded by the crops in the irrigated area, whereas irrigation water withdrawal is defined as the actual amount of water withdrawn from rivers for irrigation use. Irrigation water loss is part of irrigation water withdrawal and is defined as the amount of water lost through evaporation or seepage during transportation.

As indicated in the previous section, most of the streamflow originates from snow melt, glacier melt, and orographic rainfall in the mountainous area around the TRB. Zhang *et al.* (2013) established a modeling scheme across the Tibetan Plateau (TP) by linking the VIC model with a degree-day glacier-melt scheme. The glacier area vs. volume relationship used was mostly derived from the field measurements in TP. It is not clear whether this relationship is suitable to our study area. Besides, meteorological data uncertainties and its impact on land surface hydrology model simulations including melt water estimations are probably the primary limitation because of the scarcity of meteorological stations over the mountainous area in the TRB. Thus, we applied the observed discharge as part of the routing model inputs instead of the runoff simulated by the VIC model from the headwater basins. Hence, we can focus on the area between the observation gauges in the upstream (Table 1) and the Alaer gauge. Furthermore, we can effectively estimate and understand the impact of irrigation on surface water fluxes in these areas.

RESULTS

Model performance

Unlike the water that flows from the mountainous area, the amount of runoff generated in the irrigated area downstream is negligible because of the extremely limited rainfall and intensive evapotranspiration. Therefore, it does not affect the discharge. For this reason, the VIC model parameters that describe the hydrological properties of the soil are directly obtained from the global setup presented by Nijssen *et al.* (2001) without adjustment. Instead, the parameters for the irrigation scheme were calibrated manually and focused on irrigation water withdrawals. The depth of the top soil layer D_1 (m) in the irrigated area and the effective utilization coefficient C_u are selected as the two calibrated parameters. Both values should govern the irrigation process. Based on the discharge observed at the Alaer gauge, which is located on the main stem of the Tarim River, the model performance was evaluated in terms of the Nash and Sutcliffe efficiency (NSE) and root mean square error (RMSE). It is defined as follows:

$$\mathrm{NSE} = 1 - \frac{\Sigma(Q_{\mathrm{obs}} - Q_{\mathrm{sim}})^2}{\Sigma(Q_{\mathrm{obs}} - \bar{Q}_{\mathrm{obs}})^2} \quad (-\infty < \mathrm{NSE} < 1), \tag{1}$$

$$\mathrm{RMSE} = \sqrt{\frac{\Sigma(Q_{\mathrm{obs}} - Q_{\mathrm{sim}})^2}{n}} \quad (\mathrm{RMSE} > 0), \tag{2}$$

where Q_{obs} is the observed monthly mean discharge; Q_{sim} is the simulated monthly mean discharge; and n is number of observations during the calibration period that lasted from 1965 to 1985.

This case involves the calibration of a two-parameter model, whose NSE response surface has a global optimum region at approximately ($C_u = 0.40$, $D_1 = 0.75$ m; Figure 4(a)). This feature can be also detected on the RMSE response surface (Figure 4(b)). This result is clear and helps determine the parameter sets used to run the model. It is also well-aligned with that of an investigation of a typical irrigated area by Zhou *et al.* (2000), which indicates that the effective utilization coefficient of surface water in the Tarim River ranges from 0.40 to 0.43.

Irrigation impacts on surface water fluxes

The model was initially run without an irrigation scheme or reservoir module. Figure 5(a) shows the annual average discharge at the Alaer hydrometric gauge, which is located on the upper reach of the main stem Tarim River, whereas Figure 5(b) depicts its monthly mean. The observed

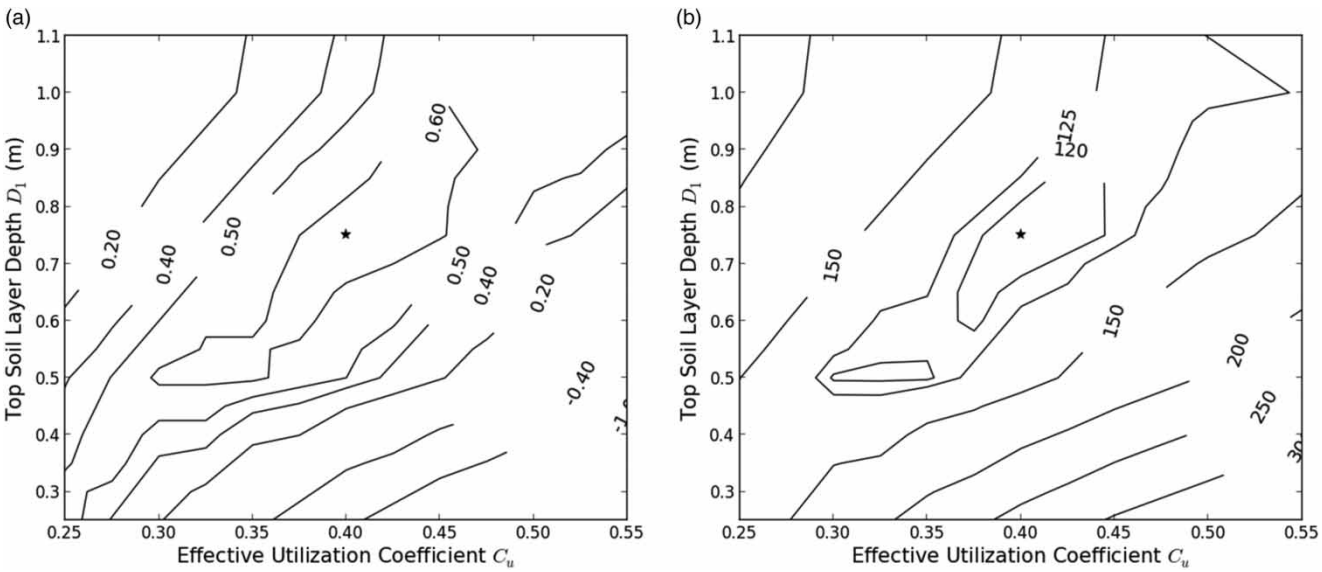

Figure 4 | Contour plots for the calibrated model parameters: (a) NSE; (b) RMSE.

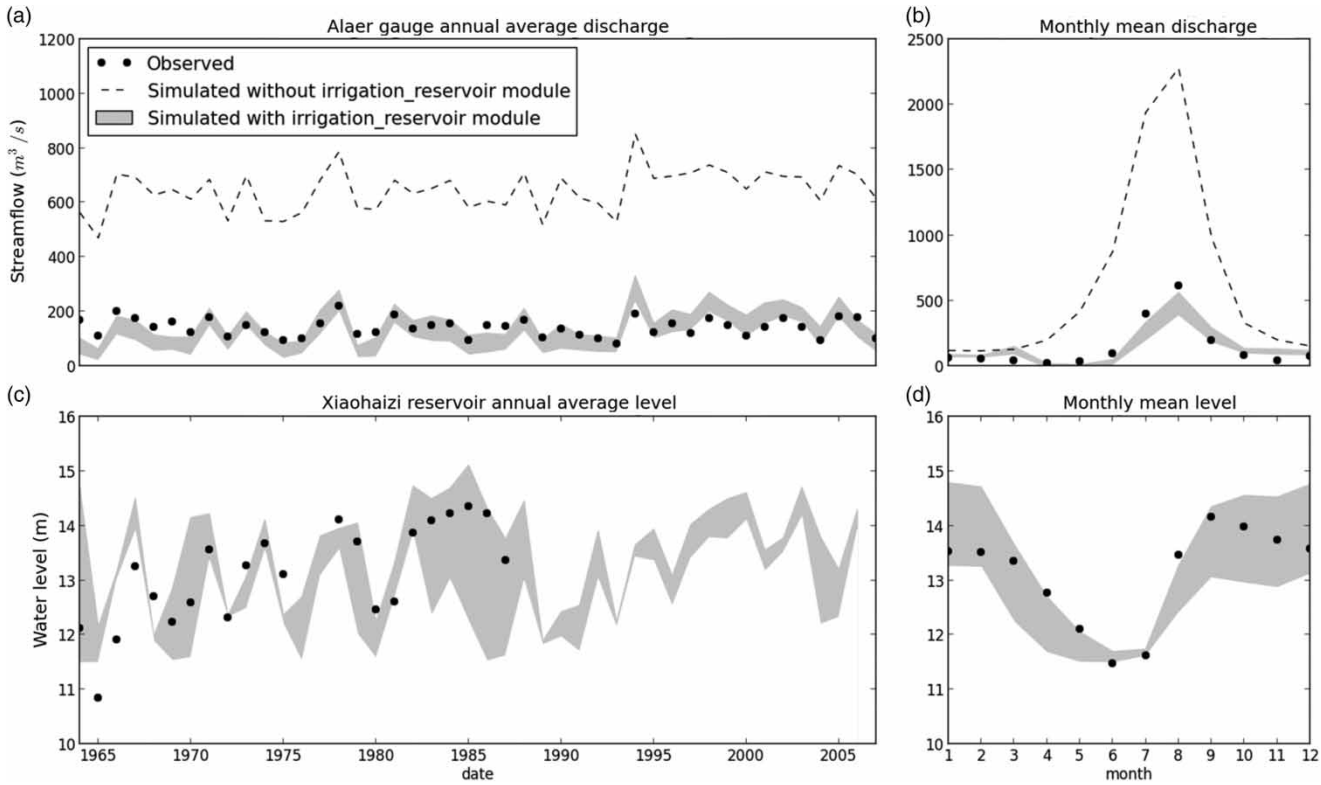

Figure 5 | (a) Annual average discharge at the Alaer gauge; (b) monthly mean discharge at the Alaer gauge; (c) annual average water level at the Xiaohaizi reservoir; (d) monthly mean water level at the Xiaohaizi reservoir.

discharge (dot) is significantly lower than that simulated in the model (dashed line). This difference implies that the combined effect of irrigation activities and reservoir operations is strengthened above this site. The model was then run with the irrigation scheme and reservoir module. Figure 5 suggests that the ranges of discharge simulation uncertainty (lightly shaded region) correspond to the model runs with the best parameter sets (NSE > 0.60 and RMSE < 125). A visual inspection of the two plots reveals that the model behavior is highly consistent with the observations, as expected. Thus, much of the surface water (70–75% based on the model simulation) is extracted from our study area for irrigation. Figure 5(c) displays the annual average water level of the Xiaohaizi Reservoir, which is situated at the middle reach of the Yarkant River with main purpose of irrigation. Figure 5(d) shows the monthly mean. The regulation effect of the reservoir on the streamflow is effectively captured by the model.

Figure 6 exhibits the spatial differences between the simulations with and without irrigation impacts in the area between the observing hydrometric gauges in the upstream and the Alaer hydrometric gauge. The left panel shows the annual average irrigation water withdrawal, runoff, evapotranspiration, and soil moisture per grid cell area without irrigation impacts, whereas the right panel shows these variables under irrigation impacts. Differences in the simulation results indicate that as a result of the irrigation impact, evapotranspiration increases much more significantly than runoff does. Notably, all numbers reported in Figure 6 are averaged over grid cells, and the significance of the differences increase if reported at an increased spatial resolution. This result implies that the operation of the canals and aqueducts remain far from effectively satisfying the irrigation water demands because of their poor construction and maintenance. In fact, the intense evaporation and seepage from these structures results in the greatest waste of surface water. As a result, the volume of water diverted into the main stem drops sharply. Thus, the lower reaches of the Tarim River began to dry up during the 1970s, and the terminal lakes Lopnor and Taitema vanished. This

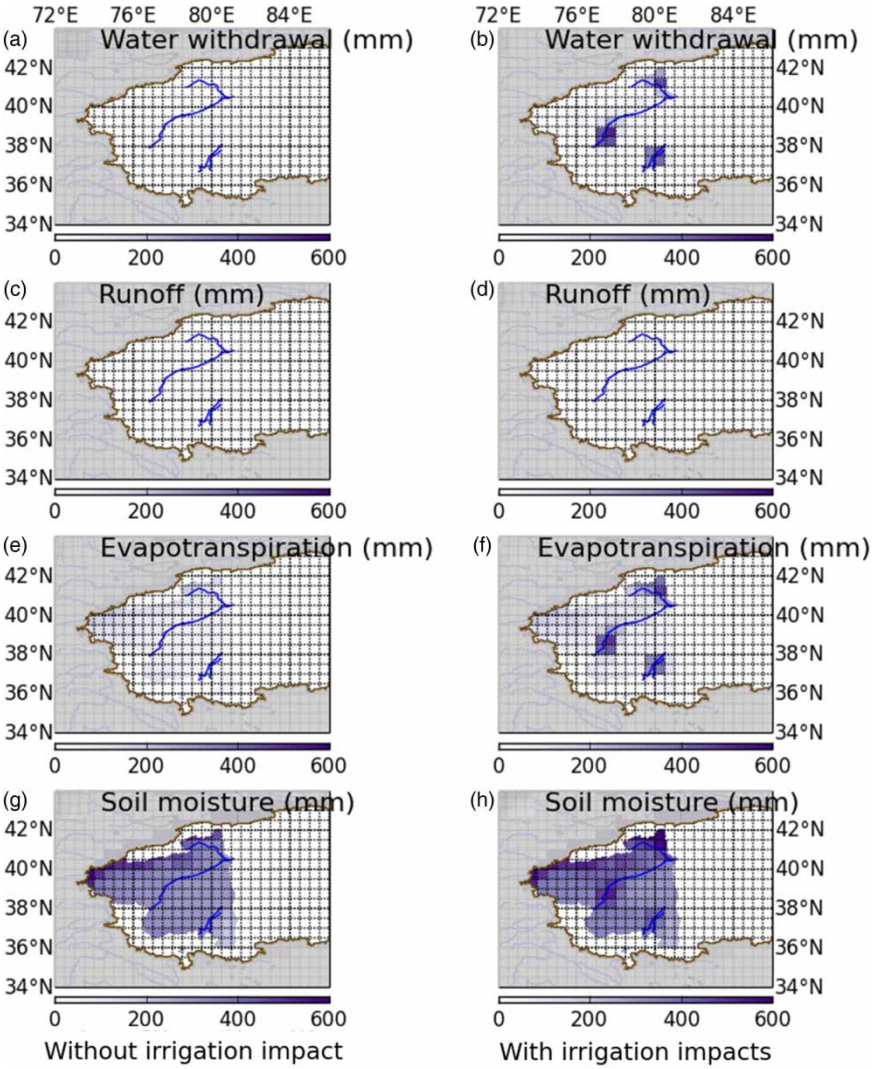

Figure 6 | Spatial effects of irrigation on surface water fluxes and states.

scenario severely degraded the natural riparian vegetation in these areas.

Change in irrigation water withdrawals

The total discharge of four headstreams increased significantly since the 1960s. However, the volume of runoff that was diverted into the main stem of the Tarim River has decreased continuously since then (Tao *et al.* 2011). These detected trends can be explained by climatic changes and, more importantly, by irrigation and related activities. In this section, we evaluate the irrigation withdrawals in the Aksu River, Hotan River, and Yarkant River based on the model simulation.

Figure 7(a) exhibits the decadal irrigation water withdrawals in three headwater basins from the 1960s to 2000s. The increasing irrigation water withdrawals have canceled out the increasing total discharge of the four headstreams since the 1960s. Thus, the amount of water flowing into the main stem of the Tarim River decreases as well (Tao *et al.* 2011). This condition can be explained by the rapid expansion of cultivated land for the massive cotton production that began in the 1990s. Irrigation water withdrawals are intensified by the increasing cropping demand from the irrigated area and by the considerable losses from the canals and aqueducts. The Tarim River is a typical inland river without its own runoff yield, and its water resources are sourced completely

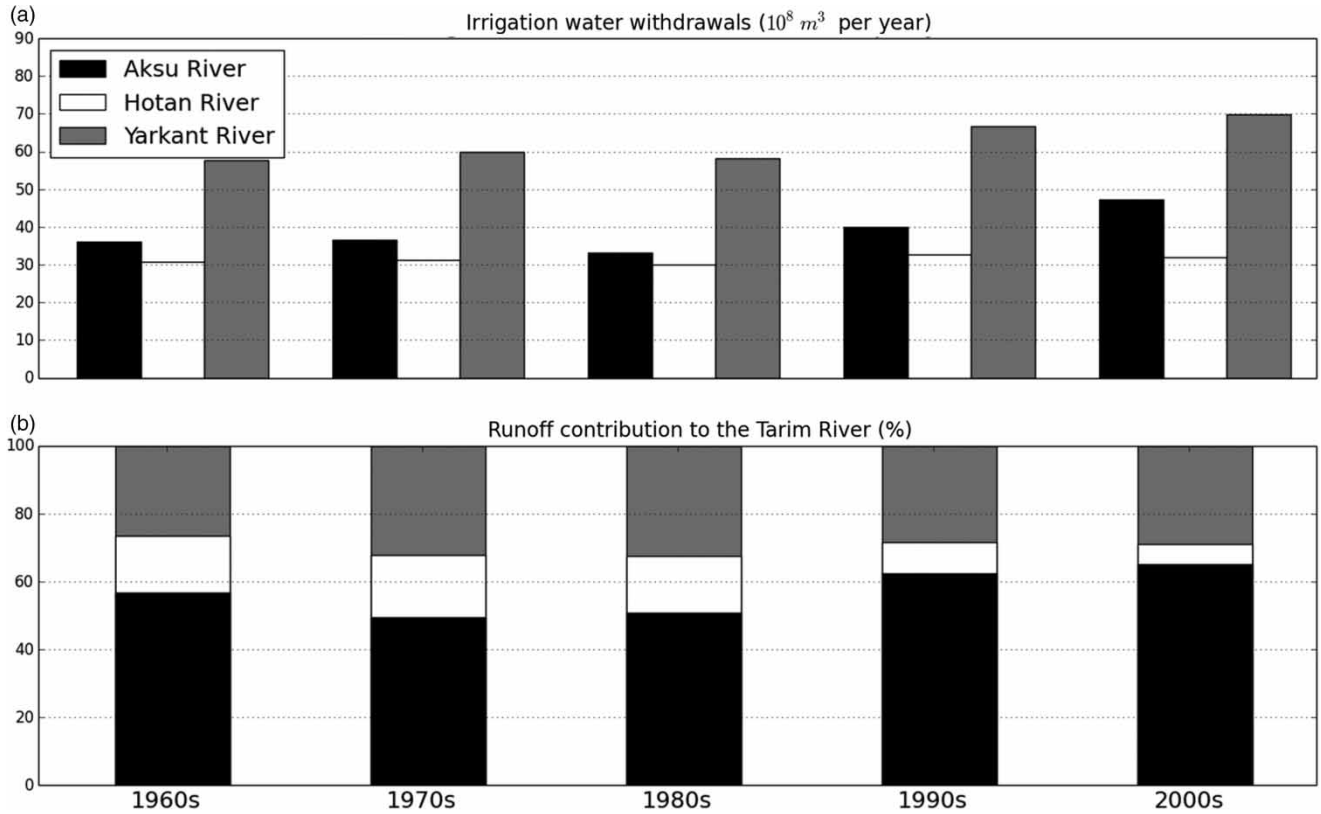

Figure 7 | (a) Annual irrigation water withdrawal from the 1960s to the 2000s; (b) variation in runoff contribution from three headwater streams to the main stem of the Tarim River.

from the headwater streams. Figure 7(b) illustrates the variation in runoff contribution from three headwater streams to the main stem. The active contribution of the Aksu River to the runoff (higher than 60%) of the main stem increases because of the significant increase in water obtained from its source area (Zhang *et al.* 2010) and its irrigation demand, which is lower than that of Yarkant River.

DISCUSSION AND CONCLUSIONS

This study developed a grid-based land surface hydrologic model coupled with an irrigation scheme and reservoir module to simulate multiple components of surface water fluxes for the driest region in China. The model was implemented at half degree in the TRB. To factor in the irrigation water losses from the canals and aqueducts as a result of their poor quality, we improved the irrigation scheme through a generalization. In the improved version of irrigation scheme, we estimate irrigation water demands, actual water withdrawals, and water losses simply by prescribing an effective utilization coefficient of the extracted surface water. We consider that the utilization coefficient of surface water should vary over time and space. Therefore, physical canals and aqueducts should be explicitly included, although this inclusion remains somewhat impractical because of poor data availability in the study area.

Although irrigation is the main cause of water loss along the river reach, other possible reasons have not been explored in this study. For example, our present modeling scheme does not include groundwater recharge and groundwater withdrawal, both of which seem to be important in the lower reaches. Moreover, the model cannot simulate the domestic use and grazing demand associated with population growth and economic development. The Kaidu River transports water to the irrigation area of the lower reaches of the Tarim River from Bosten Lake, and the amount of the transported water sometimes could be significant. However, due to data scarcity and security, we could only collect the observed discharge data in the upstream (above the Alaer gauge). Therefore, our

modeling scheme is established with focus on the area between the observing hydrometric gauges and the Alaer gauge, without the Bosten Lake included. All of these factors render our results uncertain and deserve additional attention in the design of future modeling and prediction work.

Using the land surface hydrologic model coupled with a modified irrigation scheme and reservoir module, we presented a physically based approach to evaluate the human impacts on the streamflow of the Tarim River. This streamflow at the main stem of this river has decreased in the past few decades. Our key findings are as follows. (a) We conclude that the combined effect of irrigation activities and reservoir operation is prominent upstream of the basin, from which 70–75% of the surface water is extracted for irrigation use. This condition can largely be attributed to the significant amount of water losses as a result of evaporation and the seepage of the canals and aqueducts when the effective utilization coefficient of the extracted surface water drops to approximately 0.40. The waste of extracted surface water severely reduces the water volume flowing to the main stem, therefore jeopardizing the environmental and ecological health in that area. (b) Although the total discharge of the headwater basins in the mountains has increased significantly since the 1960s, the amount of water flowing into the main stem of the Tarim River still displays a downward trend primarily as a result of increasing irrigation water withdrawals associated with the recent rapid expansion of the cultivated land. Moreover, the Aksu River contributes more actively to the runoff (higher than 60%) of the Tarim River than the Yarkant River and Hotan River do. The Tarim River only receives water from its headwater streams; thus, these findings have important implications for water resource management, agricultural development, and environmental protection in this arid region, as well as for similar river basins in which irrigation and hydraulic projects dominate the surface water fluxes.

ACKNOWLEDGEMENTS

The work presented in this paper was financially supported by the National Basic Research Program of China (grant no. 2010CB951101), the National Natural Science Foundation of China (grant no. 41101015 and 41371047), the Special Fund of State Key Laboratory of Hydrology-Water Resources and Hydraulic Engineering (1069-50985512) and the PhD Jointly Training Program from the China Scholarship Council (201206710030). The authors are very grateful to Professor Dennis Lettenmaier at the University of California, Los Angeles, and Dr Bart Nijssen at the University of Washington for their guidance and assistance.

REFERENCES

Boucher, O., Myhre, G. & Myhre, A. 2004 Direct human influence of irrigation on atmospheric water vapour and climate. *Clim. Dynam.* **22** (6–7), 597–603.

Chen, Y., Xu, C., Hao, X., Li, W., Chen, Y., Zhu, C. & Ye, Z. 2009 Fifty-year climate change and its effect on annual runoff in the Tarim River Basin, China. *Quat. Int.* **208** (1), 53–61.

de Rosnay, P., Polcher, J., Laval, K. & Sabre, M. 2003 Integrated parameterization of irrigation in the land surface model ORCHIDEE. Validation over Indian Peninsula. *Geophys. Res. Lett.* **30** (19), 1986–1990, doi:10.1029/2003GL018024.

Döll, P. & Siebert, S. 2002 Global modeling of irrigation water requirements. *Water Resour. Res.* **38** (4), 8–1.

Fekete, B. M., Wisser, D., Kroeze, C., Mayorga, E., Bouwman, L., Wollheim, W. M. & Vörösmarty, C. 2010 Millennium ecosystem assessment scenario drivers (1970–2050): climate and hydrological alterations. *Global Biogeochem. Cycles* **24** (4), GB0A12, doi:10.1029/2009GB003593.

Haddeland, I., Lettenmaier, D. P. & Skaugen, T. 2006a Effects of irrigation on the water and energy balances of the Colorado and Mekong river basins. *J. Hydrol.* **324** (1), 210–223.

Haddeland, I., Skaugen, T. & Lettenmaier, D. P. 2006b Anthropogenic impacts on continental surface water fluxes. *Geophys. Res. Lett.* **33** (8), L08406.

Haddeland, I., Heinke, J., Biemans, H., Eisner, S., Flörke, M., Hanasaki, N., Konzmann, M., Ludwig, F., Masaki, Y., Schewe, J., Stacke, T., Tessler, Z., Wada, Y. & Wisser, D. 2013 Global water resources affected by human interventions and climate change. *PNAS* **111** (9), 3251–3256.

Hao, X., Chen, Y., Xu, C. & Li, W. 2008 Impacts of climate change and human activities on the surface runoff in the Tarim River Basin over the last fifty years. *Water Resour. Manage.* **22** (9), 1159–1171.

Liang, X., Lettenmaier, D. P., Wood, E. F. & Burges, S. J. 1994 A simple hydrologically based model of land surface water and energy fluxes for general circulation models. *J. Geophys. Res. Atmos.* **99** (**D7**), 14415–14428.

Liang, X., Wood, E. F. & Lettenmaier, D. P. 1996 Surface soil moisture parameterization of the VIC-2L model: Evaluation and modification. *Glob. Planet. Change* **13** (1), 195–206.

Liu, Y. & Chen, Y. 2006 Impact of population growth and land-use change on water resources and ecosystems of the arid Tarim River Basin in Western China. *Int. J. Sustain. Dev. World Ecol.* **13** (4), 295–305.

Lohmann, D., Raschke, E., Nijssen, B. & Lettenmaier, D. P. 1998 Regional scale hydrology: I. Formulation of the VIC-2L model coupled to a routing model. *Hydrol. Sci. J.* **43** (1), 131–141.

Monteith, J. 1965 Evaporation and environment. *Symp. Soc. Exp. Biol.* **19**, 205–234.

Nijssen, B., O'Donnell, G. M., Lettenmaier, D. P., Lohmann, D. & Wood, E. F. 2001 Predicting the discharge of global rivers. *J. Clim.* **14** (15), 3307–3323.

Postel, S. L. 2000 Entering an era of water scarcity: the challenges ahead. *Ecol. Appl.* **10** (4), 941–948.

Sheffield, J., Goteti, G. & Wood, E. F. 2006 Development of a 50-year high-resolution global dataset of meteorological forcings for land surface modeling. *J. Clim.* **19** (13), 3088–3111.

Shiklomanov, I. A. & Rodda, J. C. 2003 *World Water Resources at the Beginning of the Twenty-first Century*. Cambridge University Press, Cambridge.

Siebert, S., Döll, P. & Hoogeveen, J. 2002 *Global Map of Irrigated Areas Version 2.1*. Center for Environment System Research, University of Kassel, Germany.

Tao, H., Gemmer, M., Song, Y. & Jiang, T. 2008 Ecohydrological responses on water diversion in the lower reaches of the Tarim River, China. *Water Resour. Res.* **44** (8), W08422.

Tao, H., Gemmer, M., Bai, Y., Su, B. & Mao, W. 2011 Trends of streamflow in the Tarim River Basin during the past 50 years: Human impact or climate change? *J. Hydrol.* **400** (1), 1–9.

Thevs, N. 2011 Water scarcity and allocation in the Tarim Basin: decision structures and adaptations on the local level. *J. Curr. Chin. Aff.* **40** (3), 113–117.

Vörösmarty, C. J., Green, P., Salisbury, J. & Lammers, R. B. 2000 Global water resources: vulnerability from climate change and population growth. *Science* **289** (5477), 284.

Vrugt, J. A., Gupta, H. V., Bouten, W. & Sorooshian, S. 2003 A Shuffled Complex Evolution Metropolis algorithm for optimization and uncertainty assessment of hydrologic model parameters. *Water Resour. Res.* **39** (8), 1201.

Xu, Y., Gao, X., Shen, Y., Xu, C., Shi, Y. & Giorgi, F. 2009 A daily temperature dataset over China and its application in validating a RCM simulation. *Adv. Atmos. Sci.* **26** (4), 763–772.

Xu, Z., Liu, Z., Fu, G. & Chen, Y. 2010 Trends of major hydroclimatic variables in the Tarim River Basin during the past 50 years. *J. Arid Environ.* **74** (2), 256–267.

Yatagai, A., Kamiguchi, K., Arakawa, O., Hamada, A., Yasutomi, N. & Kitoh, A. 2012 APHRODITE: Constructing a long-term daily gridded precipitation dataset for Asia based on a dense network of rain gauges. *Bull. Am. Meteorol. Soc.* **93** (9), 1401–1415.

Zhang, Q., Xu, C. Y., Tao, H., Jiang, T. & Chen, Y. D. 2010 Climate changes and their impacts on water resources in the arid regions: a case study of the Tarim River Basin, China. *Stoch. Environ. Res. Risk Assess.* **24** (3), 349–358.

Zhang, L., Su, F., Yang, D., Hao, Z. & Tong, K. 2013 Discharge regime and simulation for the upstream of major rivers over Tibetan Plateau. *J. Geophys. Res. Atmos.* **118** (15), 8500–8518.

Zhao, R. 1992 The Xinanjiang model applied in China. *J. Hydrol.* **135** (1), 371–381.

Zhou, H., Song, Y. & Hu, S. 2000 Irrigated agriculture and sustainable water management strategies in the Tarim Basin. In: *Proceedings of the workshop on New Approaches to Water Management in Central Asia*, Aleppo, Syria.

First received 26 November 2014; accepted in revised form 25 February 2015. Available online 13 April 2015